Report on a problem studied at the UK Mathematics-in-Medicine Study Group Keele 2012
< http://www.maths-in-medicine.org/uk/2012/transmucosal-drug-delivery/ >

Mathematical Modelling of Transmucosal Drug Delivery

Najida Begum[1],Vanessa Hearnden [2], Aniayam Okrinya [3]
Dennis Reddyhoff [3], Giles Richardson [4], John Ward [3] & Robert Whittaker [5]

[1] Pharmerit Ltd, York Science Park
[2] School of Clinical Dentistry, University of Sheffield
[3] Department of Mathematical Sciences, Loughborough University
[4] School of Mathematics, University of Southampton
[5] School of Mathematics, University of East Anglia

Problem presenter: Vanessa Hearnden

MATHEMATICS IN MEDICINE STUDY GROUP
KEELE UNIVERSITY 2012

Abstract

Transmucosal drug delivery across the oral mucosa is an attractive drug delivery route with a number of advantages over commonly used delivery methods (including injections). It is accessible, enables delivery directly into the blood stream (without passing via the liver) and is capable of sustained prolonged drug delivery. In order to develop successful transmucosal systems the properties which affect the diffusion of drugs across the epithelium must be better understood. It is known that lipophilicity plays an important role in permeability however the precise effect of hydrophilicity and lipophilicity are not well understood. Here we present a coupled non-linear PDE system which has been developed to predict the parameters which affect drug permeability as a function of lipophilicity. This model considers the different layers which the epithelium is comprised of and the relative importance of each layer. The model is able to predict qualitatively data profiles of drug delivery through lipophilic particles (spatial and temporal evolutions) reported by experimental data. The model has many limitations and future development of the model should consider drug internalisation by cells and long term experimental data that has the ability to validate the current model for varying lipophilicity within the epithelial tissue. The current assumptions surrounding the model may need some re-consideration to better understand the profiles seen experimentally.

1 Introduction

The oral mucosa is the epithelial lining of the oral cavity, which includes the tongue, cheeks, palate and gums. The oral mucosa is a multi-layered stratified squamous epithelium comprised of cells called keratinocytes (which bear similarities to the structure of the skin). Within the oral epithelium several layers of keratinocytes are contained with a cell thickness between 100-300μm. The basal keratinocytes divide and replenish cells above to maintain a healthy epithelium. During the keratinisation process as cells move towards the surface they differentiate and change their behaviour and composition (refer to Figure 1). The most superficial cells of the epithelium are terminally differentiated cells and in some areas of the oral cavity, such as the hard palate and tongue, this layer is keratinised. Beneath the superficial cells lies the granular cell layer. These cells are predominantly responsible for the permeability barrier of the oral mucosa. Beneath this layer is the spinous cell layer, containing supra-basal cells while the deepest layer of the epithelium is the basal cell layer. These basal cells are undifferentiated, highly proliferative cells and are responsible for regenerating the epithelium. The basal cells lie on the basement membrane which is a mixture of proteins including collagen IV and laminin. Beneath the basement membrane lies the connective tissue, a hydrated mesh of proteins containing fibroblasts (cells responsible for producing extra-cellular matrix proteins), immune cells and a blood supply. Figure 1 presents the structure of the oral mucosa and keratinisation process described above.

The oral mucosa and the skin have many structural similarities where both epithelial tissues play a crucial role as a barrier against exogenous substances, pathogens and mechanical stress. However both types of tissue are distinct from one another as they perform different functions in the body. For example, the oral mucosa remains hydrated by saliva while the skin provides a water-proof barrier and the most superficial layer is highly keratinised. The oral mucosa is 4-4000 times more

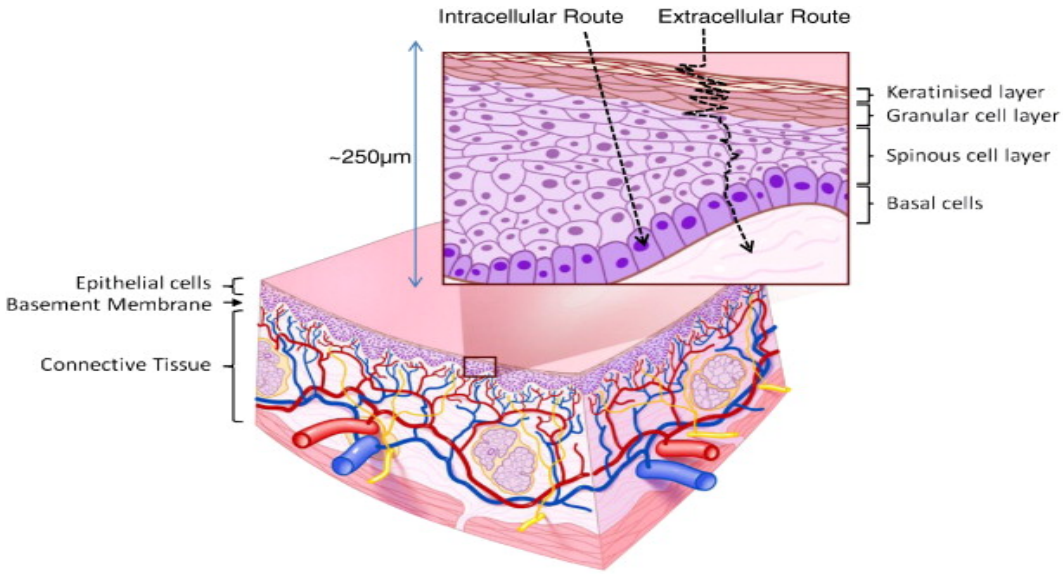

Figure 1: Structure of the oral mucosa and the keratinisation process

permeable compared to the skin depending on the substance considered.

1.1 Trans-mucosal drug delivery

The oral mucosa provides a unique opportunity to deliver drugs into the bloodstream thereby avoiding the harsh environment of the gastro-intestinal (GI) tract and first pass metabolism in the liver that prevent many drugs from being delivered orally (eg. via tablets and syrups) [1]. The oral mucosa has several features which make it an ideal site for drug delivery. The oral cavity is well hydrated aiding in the solubility of drugs and it is easily accessible for self administration. The oral mucosa repairs itself quickly and is well vascularised making entry into the bloodstream rapid and direct. Unfortunately, there are also limitations to this method of drug delivery method, most importantly the permeability barrier.

The oral mucosa is a protective tissue designed to prevent unwanted materials such as pathogens from entering the body and keeps the underlying tissue hydrated by preventing fluid loss. This same permeability barrier hinders the permeation of drugs across the oral epithelium and the level of hinderance is dependent on the drugs properties. The permeability barrier is predominantly found in the lipid rich upper layers of the epithelium (granular layer). The supra-basal cells have strong desmosomal junctions and form membrane coating granules, which are lipophilic and are released into the extracellular space. This enhances keratinocyte adhesion but also slows the passage of hydrophilic materials. However, different areas of the mouth display different levels of permeability barrier. The area below the tongue (floor of mouth) has a thin epithelium that is significantly more permeable than other areas of the oral mucosa, making it an ideal site for drug delivery. Figure 1 presents the intracellular and extra-cellular routes of drug delivery through the oral mucosa.

1.1.1 Transmucosal treatments available and under investigation

Drugs which are currently delivered via the trans-mucosal route include glyceryl trinitrate for angina pectoris, opioid analgesics for rapid pain release and midazolam for seizures [10]. In addition to these, an insulin oral spray is currently in Phase III clinical trials [11] and a nicotine oral spray is now commercially available [12]. It is particularly desirable to develop transmucosal delivery systems and formulations for drugs which are poorly delivered via tablets and syrups. This includes drugs which have low bioavailability as a result of the first pass effect or degradation in the GI tract, drugs which are currently administered via injection and/or drugs which have failed to gain approval as a result of inadequate bioavailability.

2 MMSG

2.1 Problem presented by Vanessa Hearnden

Drugs which cannot be delivered via the oral route (tablets and syrups) are most often administered by parenteral routes (injections). While injections are practical for single doses an alternative deliv-

ery method is desirable where repeated treatment is required for chronic diseases. The parenteral routes are expensive as it requires health care providers and is not well accepted by patients.

2.2 Modelling approach and limitations

In order to utilise the trans-mucosal route for drug delivery it is important to understand the barriers to drug permeability and the properties which are most crucial for optimal drug delivery. Understanding the drug properties which affect diffusion will enable researchers to design drugs which can better diffuse and develop delivery systems for suitable drugs. It will also aid in identifying drugs which are suitable for this method of delivery. Here we aim to model mathematically the effect drug properties (namely lipophilicity) have on diffusion across the oral mucosa (explained in further details below).

2.3 Drug permeability

There are large amounts of data available regarding the permeability of drugs across the skin, and there are several mathematical models available to predict trans-dermal permeability, reviewed here [3] [1]. By comparison little is known about the materials which most easily cross the oral mucosa. While some of the features of the skin permeability presented in existing mathematical models are adaptable to the oral mucosa, the stratum corneum of the skin, which is the predominant rate limiting step, is not present in most areas of the oral mucosa as there is far less keratinisation. There are a number of studies which have looked at the permeability of select compounds across the oral mucosa: dextran [4], tritiated water [6], horseradish peroxidase [7], TGF-β3 [8] and various chemical markers [9] however extensive studies on a wide range of compounds have not been conducted.

The permeability of a drug across the oral mucosa will be dependent on: the lipophilicity of the drug, the molecular weight of the drug, the probability of the drug binding to proteins or cells within the oral mucosa and the charge or ionisation of the drug. Compounds which have small molecular weight, good lipid solubility and non-ionised species are believed to be the most easily diffusible [2]. However, the relative importance of each of these factors and the optimum range of each parameter is yet to be elucidated. Other important practical factors include the susceptibility of drugs to be degraded by enzymes in the oral cavity, the solvent used to solubilise the drug prior to administration, the medium used to deliver the drug (paste, gum, spray, patch, lozenge or gel) and the concentration of drug at administration. Designing the ultimate transmucosal treatment will be a trade off between drug efficacy, permeability through the epithelium and solubility in the bloodstream; information on the relative importance of compound properties will be crucial.

2.3.1 Lipophilicity and drug permeability

Lipophilicity is the measure of a materials solubility in lipids or fats. The opposite to lipophility is hydrophilicity (how soluble something is in water). The lipid rich regions of the epithelium slow

[1] From a modelling perspective it should be noted that whilst current diffusion skin models may be part useful for the investigation of trans-mucosal drug delivery, the differences between the two types of tissue should also be acknowledged.

the passage of hydrophilic materials as they preferentially remain in the water rich regions and find it energetically unfavourable to pass into the lipophilic regions. It is generally accepted that if a drug is too hydrophilic it will be unable to pass across the epithelium in high enough quantities to be therapeutically beneficial. On the other hand if a drug is too hydrophobic it will not be soluble in the hydrophilic regions of the epithelium, so will not leave the formulation easily and will not be soluble in the blood stream if it reaches the connective tissue and blood supply.

2.4 Key publication: Hoogstraate 1996

The Hoogstraate paper investigated an experiment involving the distribution of Fluorescein isothiocyanate (FITC) across a porcine buccal epithelium of a given thickness with different layers that could be hydrophilic, lipophilic or mixed. They assume that the distribution of a substance across a membrane is usually determined by diffusion and partitioning processes.

The experiment considered two chambers which were set up with the mucosa between them, the drug was then deposited in one chamber and its progress through the mucosa was measured. The experiment lasted two hours with measurements taken every 5 minutes. The first graph presented in Figure 2 (a) reports the average fluorescence intensity at differing positions in the mucosa measured at 5 minute intervals, the higher the fluorescence, the greater the drug availability in that particular area of the epithelium. The second graph presented in Figure 2 (b) illustrates the average fluorescence intensity against time at a given position within the epithelial tissue.

The proposed mathematical approach will consider these graphs to check the model and its ability to reproduce the behaviour of experimental data presented in this paper. Model prediction of the large "gaps" between consecutive measurements will imply that the proposed kinetics across the differing boundary compositions was accurate (for example the behaviour in the Figure 2 (b) around the $t \approx 2000$ mark).

The following sections will detail the proposed mathematical model to exemplify the drug delivery through the differing mediums and composition found in the oral mucosa, the choice of parameters chosen and extracted from Hoogstraate et al (1996) and comparisons between the numerical simulations and experimental data (presented Figure 2 (a) and (b)).

(a)

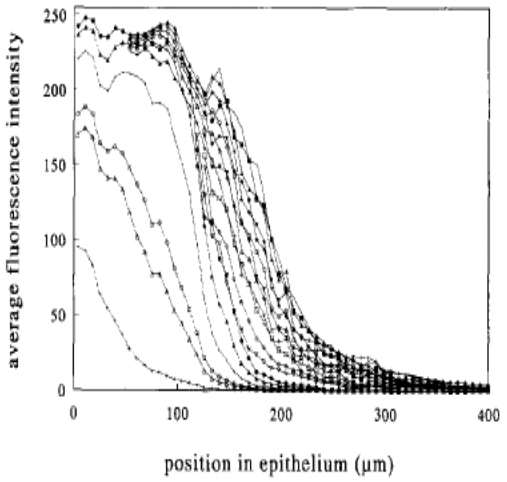

Fig. 4. The average fluorescence intensity of FITC in buccal epithelium versus the position in the epithelium. The difference between consecutive curves is 5 min. The far left curve represents the situation after the first 5 min.

b)

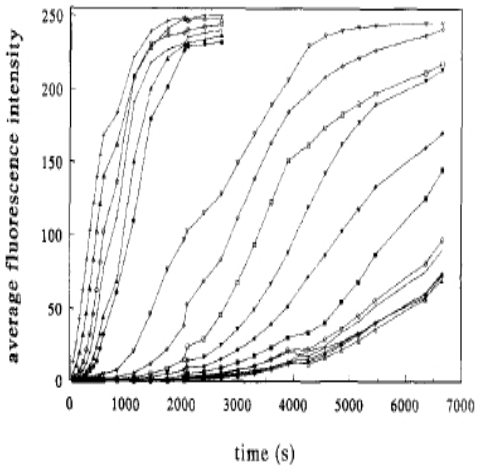

Fig. 5. The average fluorescence intensity of FITC in buccal epithelium versus diffusion time. The difference between consecutive curves is 20 μm, the far left curve being the surface layer of the epithelium.

Figure 2: Plots of showing the infiltration of fluorescent, highly lipophilic particles into epithelial tissue. (a) Shows the spatial evolutions of particles and (b) shows the concentration evolution at equally spaced distances from epithelial layer surface [5].

3 Mathematical Modelling

In this section we present a mathematical model that defines the delivery of drugs entering oral cavity and diffusing through the hydrophillic, lipophillic (lipid rich) and mixed layers (mix of lipid rich and aqueous fluid) within the epithelial tissue.

3.1 Model assumptions

To model drug delivery we take into account the structure of the oral mucosa where composition of the differing layers within this medium will affect the drug permeability and the experimental data we have seen in Hoogstraate et al (1996). The following modelling assumptions apply here:

- The drug enters the oral cavity and diffuses through the epithelium into the connective tissue where the blood stream lies.
- There is linear diffusion in each component of of each layer with degradation of the drug over time.

Table 1: Variables and parameters appearing in the governing equations

Parameters	Description
a	Thickness of the mixed layer
$2d$	Thickness of the lipid layer
γ^2	Partitioning rate constant
P	Partitioning coefficient
b_{et}	The surface area of lipid/ water (aqueous) interface per unit volume of tissue
$\mathcal{B}_L$	Permeability of the lipid layer
$\mathcal{B}_L$	Permeability of the water (aqueous) layer
K_L	Permeability in the lipid media of the mixed layer
K_W	Permeability in the water (aqueous) media of the mixed layer
D_W	Diffusion coefficient of water (aqueous media) in the mixed layer
D_F	Diffusion coefficient within the lipid layer
D_L	Diffusion coefficient of lipids in the mixed layer
D_e	Effective diffusion coefficient in the mixed layer
c_D	Drug concentration in the oral cavity
c_F	Drug concentration in the lipid layer
c_L	Drug concentration in the lipid medium within the mixed layer
c_W	Drug concentration in the water (aqueous media) within the mixed layer
λ	Degradation rate
ϕ_L	Volume fractions of the substance in lipids
ϕ_W	Volume fraction of the substance in water (aqueous media)

- Transfer between components in the mixed layers is proportional to the distance from equilibrium.
- There is continuity of concentrations and fluxes between the compartments of the oral mucosa (refer to the model schematic presented in Figure 3).

The parameters considered for our model are mainly partitioning and diffusion obtained from Hoogsstraate's et al (1996). We denote the thickness of the mixed layer by a and that of the lipid layer by $2d$. One significant finding from the experiment we consider in our model is the fluorescent rate limiting intermediate strata. The paper suggests that a mathematical model aimed at determining the concentration profile of FITC or other related substances across a membrane should include calculation of regionally specific diffusion coefficients as this would enhance identification of the rate limiting intermediate layer. The model schematic is presented in Figure 3 illustrates the layers defined in the mathematical model (to resemble the structure of the oral mucosa). The list of parameters and variables considered in the model are presented in Table 1.

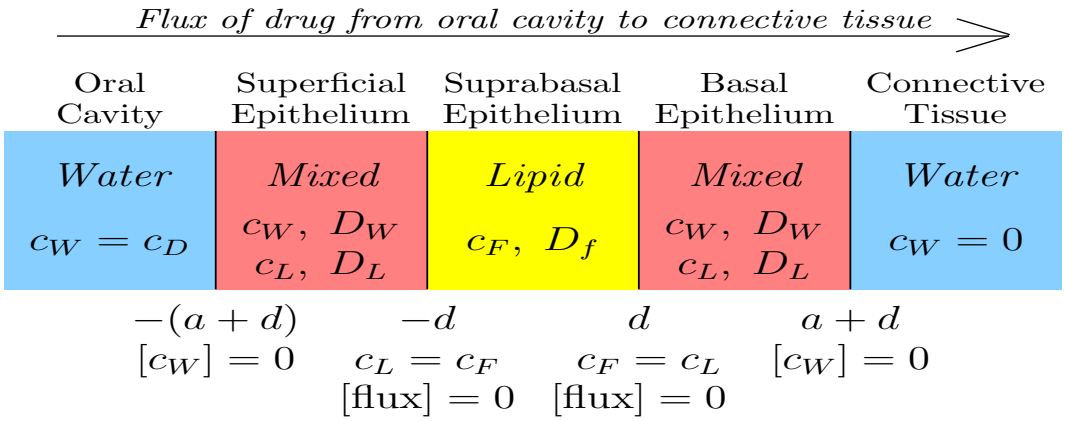

Figure 3: Model schematic of the oral mucosa

3.2 Model equations

The lipid rich layer $-d < x < d$. Here the diffusion of drug is almost entirely through the lipid and as such its concentration in the lipid c_F is described by a single diffusion equation

$$\frac{\partial c_F}{\partial t} = \frac{\partial}{\partial x}\left(D_F \frac{\partial c_F}{\partial x}\right) - \lambda c_F \tag{1}$$

where we include a term $-\lambda c_F$ to model the degradation of the drug over time.

The mixed layers $-(a+d) < x < -d$ and $d < x < a+d$. Here the diffusion of drug takes place through a matrix of lipid rich matter bathed in an aqueous fluid and so we should consider both its concentration in the lipid medium c_L and in the aqueous fluid c_W. Furthermore transfer of drug molecules takes place at the interface between the two media. A similar diffusional process to the one described here is detailed in [13]- where transfer through a microstructured material consisting of two constituents was considered in the context of lithium ion batteries. In [13], a microscopic diffusion model for lithium ions in an electrolyte, with lithium consuming reactions taking place on the surface of microscopic electrode particles, was treated by using the methods of homogenisation to yield an effective medium model applicable over the scale of the battery. The coefficients in the battery scale model are directly derivable from the microscopic diffusion model and the solution of a canonical microscale problem. From our perspective it is enough to note that the results of [13] can be readily generalised to the context of drug delivery to yield two macroscale equations for the diffusion of drug in lipid and the aqueous fluid. These take the form

$$\phi_L \frac{\partial c_L}{\partial t} = \frac{\partial}{\partial x}\left(D_L \mathcal{B}_L \frac{\partial c_L}{\partial x}\right) - b_{et}\gamma^2\left(c_L P^{-1/2} - c_W P^{1/2}\right) - \phi_L \lambda c_L \tag{2}$$

$$\phi_W \frac{\partial c_W}{\partial t} = \frac{\partial}{\partial x}\left(D_W \mathcal{B}_W \frac{\partial c_W}{\partial x}\right) + b_{et}\gamma^2\left(c_L P^{-1/2} - c_W P^{1/2}\right) - \phi_W \lambda c_W \tag{3}$$

where ϕ_L and ϕ_W are the volume fractions of the lipid and aqueous media, respectively; $\mathcal{B}_L$ and $\mathcal{B}_W$ are the permeability of the lipid medium and aqueous medium, respectively; and b_{et} is the

surface area of lipid/aquoues interface per unit volume of tissue. The permeabilities of the two materials represent the degree of extra difficulty that the drug finds in diffusing along the necessarily convoluted paths in either medium. They are defined such that if microstructure significantly impedes diffusion $0 < \mathcal{B} \ll 1$ whereas if it provides virtually no additional diffusion $\mathcal{B} \approx \phi$ and in general $0 < \mathcal{B} < \phi$. A method for calculating the permeability from a known quasi-periodic microstructure is given in [13]. It is common, though not entirely justified, to assume that the tortuousities scale with the appropriate volume fractions of the different media so that $\mathcal{B}_L = K_L\phi_L$ and $\mathcal{B}_W = K_W\phi_W$ (for more discussion of the effect of volume fraction on permeability see [14]).

Boundary conditions on $x = -(a+d)$ and $x = a+d$. We assume that diffusion in the aqueous media in the oral cavity and the connective tissue are sufficiently fast that we can accurately approximate the concentrations there as constants, writing $c_W = c_D$ in $x < -(a+d)$ and $c_W = 0$ in $x > a+d$. Thus the appropriate boundary conditions on the outer edges of the superficial epithelium and the basal epithelium are

$$c_W|_{x=-(a+d)} = c_D \qquad \text{and} \qquad c_W|_{x=a+d} = 0. \tag{4}$$

Interface conditions on $x = \pm d$. On the interfaces between the two mixed regions and the lipid region we need to impose appropriate conditions. It is reasonable to assume that transfer of drug from one region to the other takes place almost entirely through diffusion directly between the two lipids and that the effective flux of drug in the aqueous medium at the interface is zero. It follows that there is continuity of drug concentrations in the lipid on either side of the interfaces and that the fluxes in the lipid regions are also continuous (refer to Figure 3). Mathematically these conditions can be stated as

$$c_L|_{x=-d} = c_F|_{x=-d}, \qquad D_W\mathcal{B}_W\frac{\partial c_W}{\partial x}\bigg|_{x=-d} = 0, \qquad D_L\mathcal{B}_L\frac{\partial c_L}{\partial x}\bigg|_{x=-d} = D_F\frac{\partial c_F}{\partial x}\bigg|_{x=-d}, \tag{5}$$

$$c_L|_{x=d} = c_F|_{x=d}, \qquad D_W\mathcal{B}_W\frac{\partial c_W}{\partial x}\bigg|_{x=d} = 0, \qquad D_L\mathcal{B}_L\frac{\partial c_L}{\partial x}\bigg|_{x=d} = D_F\frac{\partial c_F}{\partial x}\bigg|_{x=d}. \tag{6}$$

3.3 Model simplification in the limit of large partitioning rate

Diffusion within the lipid is always considerably slower than that in the aqueous medium. It follows that a typical timescale T for a drug molecule to diffuse from the oral cavity to the connective tissue is given by the timescale to diffuse across the superbasal endothelium, that is $T = 4d^2/D_F$. If the dimensionless number $T\gamma^2 b_{et} \gg 1$ then the exchange of drug between the lipid and aqueous phases in the mixed region is fast in comparison to other processes encapsulated in (2)-(3) such that a quasisteady state rapidly appears in which

$$c_W = P^{-1}c_L + O((T\gamma b_{et})^{-2}c_L). \tag{7}$$

We can use the above relation to eliminate c_W from (2)-(3). If we then add (2) to (3) we obtain a single equation for the average concentration $c = c_L(\phi_L + \phi_W P^{-1})$, that can be written in the

form

$$\frac{\partial c}{\partial t} = \frac{\partial}{\partial x}\left(D_e \frac{\partial c}{\partial x}\right) - \lambda c \qquad \text{in} \quad \begin{cases} -(a+d) < x < -d \\ d < x < (a+d) \end{cases} \tag{8}$$

where the effective diffusivity D_e is given by

$$D_e = \left(\frac{P D_L \mathcal{B}_L + D_W \mathcal{B}_W}{P\phi_L + \phi_W}\right). \tag{9}$$

We can identify the net drug flux as $-D_e c_x$. If we also rewrite (1) in terms of the total drug concentration (in this case $c = c_F$) we obtain the final equation in the model

$$\frac{\partial c}{\partial t} = \frac{\partial}{\partial x}\left(D_F \frac{\partial c}{\partial x}\right) - \lambda c \qquad \text{in} \quad -d < x < d. \tag{10}$$

It remains to impose continuity conditions on $x = \pm d$. Formally this requires the analysis of boundary layers about $x = -d$ and $x = d$, in which the balance $c_W = P^{-1}c_L + O((T\gamma b_{et})^{-2}c_L)$ breaks down (for details see appendix A)). However it can be readily demonstrated that the drug concentration in the lipid does not change appreciably across this layer and furthermore that the flux of drug across the boundary layer has to be continuous. This suggests that the interface conditions on our simplified model are

$$\left.\frac{c}{(\phi_L + \phi_W P^{-1})}\right|_{x=-d} = c|_{x=-d}\,, \qquad \left. D_e \frac{\partial c}{\partial x}\right|_{x=-d} = \left. D_F \frac{\partial c}{\partial x}\right|_{x=-d}, \tag{11}$$

$$\left.\frac{c}{(\phi_L + \phi_W P^{-1})}\right|_{x=-d} = c|_{x=-d} \qquad \left. D_e \frac{\partial c}{\partial x}\right|_{x=d} = \left. D_F \frac{\partial c}{\partial x}\right|_{x=d}. \tag{12}$$

The simplified model is closed by conditions at the edge of the oral cavity and the edge of the connective tissue

$$c|_{x=-(a+d)} = P c_D(\phi_L + \phi_W P^{-1}) \qquad \text{and} \qquad c|_{x=a+d} = 0. \tag{13}$$

In summary the the simplified model is comprised of equations (8) and (10), coupled via the interface conditions (11) and (12), and satisfying the boundary conditions (13).

Remark on the boundary conditions. The boundary condition (13) is determined by the concentration of drug in aqueous solution in the oral cavity c_D, and this in turn is determined by an equilibrium between the drug in the pill and the surrounding saliva. If the drug is highly lipophilic it will typically be dissolved in high concentration in a lipid formulation within the pill. However the high degree of drug lipophilicity may mean that and equilibrium of the form $c_W = P^{-1}c_L$ may not hold because the aqueous drug concentration c_W saturates. This effectively puts an upper bound on c_D as a function of drug lipophility.

4 Results

A slightly more general multi-layer model can be written in the form

$$\phi_L^i \frac{\partial c_L^i}{\partial t} = D_L^i \mathcal{B}_L^i \frac{\partial^2 c_L^i}{\partial x^2} - b_{et}^i \gamma^{i2} (P^{i\,-1/2} c_L^i - P^{i\,1/2} c_W^i) - \lambda_L^i \phi_L^i c_L^i, \tag{14}$$

$$\phi_W^i \frac{\partial c_W^i}{\partial t} = D_W^i \mathcal{B}_W^i \frac{\partial^2 c_W^i}{\partial x^2} + b_{et}^i \gamma^{i2} \left(P^{i\,-1/2} c_L^i - P^{i\,1/2} c_W^i \right) - \lambda_W^i \phi_W^i c_W^i, \tag{15}$$

where i is the layer index and W and L represent the extracellular (aqueous) fluid and lipid phases, respectively. On the assumption that equilibration of drug concentration between the water and lipid phases happens rapidly in comparison to transport and decay, we let $\gamma \to \infty$ and deduce

$$c_L \sim P\, c_W. \tag{16}$$

Adding (15) and (14) and using (16) we obtain

$$\frac{\partial c^i}{\partial t} = D_e^i \frac{\partial^2 c_W^i}{\partial x^2} - \lambda_e^i c^i. \tag{17}$$

where

$$c^i = \phi_W^i c_W^i + \phi_L^i c_L^i = (\phi_W^i + P^i \phi_L^i) c_W^i \tag{18}$$

is the mean concentration in the ith layer, and

$$D_e^i = \frac{D_W^i \mathcal{B}_W^i + P^i D_L^i \mathcal{B}_L^i}{\phi_W^i + P^i \phi_L^i} \qquad \text{and} \qquad \lambda_e^i = \frac{\phi_W^i \lambda_W^i + P^i \phi_L^i \lambda_L^i}{\phi_W^i + P^i \phi_L^i} \tag{19}$$

are the effective diffusivity and degradation rate respectively.

The boundary and initial conditions are

$$\begin{aligned}
&t = 0 && && c^i = 0, \\
&x = 0 && -D_e^1 \frac{\partial c^1}{\partial x} = Q \left(1 - \frac{P_b c^1}{\phi_W^1 + P^1 \phi_L^1} \right), && \\
&x = X_{12} && -D_e^1 \frac{\partial c^1}{\partial x} = -D_e^2 \frac{\partial c^2}{\partial x}, && \frac{c^1}{\phi_W^1 + P^1 \phi_L^1} = \frac{c^2}{\phi_W^2 + P^2 \phi_L^2}, \\
&x = X_{23} && -D_e^2 \frac{\partial c^2}{\partial x} = -D_e^3 \frac{\partial c^3}{\partial x}, && \frac{c^2}{\phi_W^2 + P^2 \phi_L^2} = \frac{c^3}{\phi_W^3 + P^3 \phi_L^3}, \\
&x = 1 && && c^3 = 0,
\end{aligned}$$

where $x = 0$ is the coordinate of skin and drug delivery device, $x = 1$ is the coordinate of skin base (assumed a perfect sink) and X_{12} and X_{23} are the coordinates of the layers' interfaces, on which continuity of flux and concentration are assumed (refer to Figure 3). The boundary conditions on the concentration at X_{12} and X_{23} result from assuming that c_W^i is continuous at those interfaces.

4.1 Parameter values

The parameters considered in the model are based on or derived from [5]. The model parameters and the corresponding values considered in the numerical simulations are presented in Table 2.

The parameters represent a "fairly" lipophilic drug $P^1 = 100$ that diffuses considerably slower in the lipid phases (diffusion coefficient 1000 times smaller). The epithelial cell volume fraction is 0.95 throughout, 80% of the extracellular space in layers 1 and 3 consists of the watery phase whilst only 2% of this space is water in layer 2. The partitioning parameter at $x = 0$ implies the drug delivery media is more lipophobic than the watery phase in the epithelium. In the simulations no degradation is assumed.

Table 2: List of values used in the simulations.

Parameter	Value	Parameter	Value
X_{12}, X_{23}	0.3, 0.8	P^1, P^2, P^3	100, $1039/49 \approx 21.2^*$, 100
$\phi_W^1, \phi_W^2, \phi_W^3$	0.04, 0.001, 0.04	$\phi_L^1, \phi_L^2, \phi_L^3$	0.01, 0.049, 0.01
D_W^1, D_W^2, D_W^3	1, 1, 1	D_L^1, D_L^2, D_L^3	0.001, 0.001, 0.001
$\lambda_W^1, \lambda_W^2, \lambda_W^3$	0, 0, 0	$\lambda_L^1, \lambda_L^2, \lambda_L^3$	0, 0, 0
Q	2	P_b	0.1
$\mathcal{B}_W^i$, $\mathcal{B}_L^i$	ϕ_W^i, ϕ_L^i	b_{et}^1, b_{et}^2, b_{et}^3	1, 1, 1

* Value computed using $P^2 = (\phi_W^1 + P^1\phi_L^1 - \phi_W^2)/\phi_L^2$ in order to satisfy (20).

4.2 Numerical Simulations

The illustrations of the experimental data reported in Hoogstraate et al (1996) and presented in Figure 2 (a) and (b) are used for comparative purposes here. From Figure 2(a) we observe a fairly monotonic descent of particle concentration. This is a little surprising given the known spatial distribution of lipid layers in the tissue, most concentrated in the central layer, and partitioning properties of drugs, we would expect a clearly elevated concentration of particles in the middle; however, this appears not to be the case. To reproduce the results shown in the figures a "careful" choice of parameters was required, more specifically we need to set

$$\phi_W^1 + P^1\phi_L^1 \;=\; \phi_W^2 + P^2\phi_L^2 \;=\; \phi_W^3 + P^3\phi_L^3. \tag{20}$$

This ensures that the mean concentrations are continuous at the interfaces, consistent with the experimental results from [5].

Furthermore, Figure 2(b) shows that the drug in the inner regions eventually reaches the same concentration as that in the tissue nearest to the drug source, suggesting that $\partial c^i/\partial x$ may also be constant in large time; if this is the case then this implies that the combined diffusion coefficient D_e^i must be uniform across the domain. In truth this is exposing limitations in the current model and probably is evidence that the drug is being internalised by cells during the experiment, a factor not considered in depth during the modelling during the study group week. Nevertheless, we will proceed with a few illustrative simulations using the parameter values listed in Table 2 (which

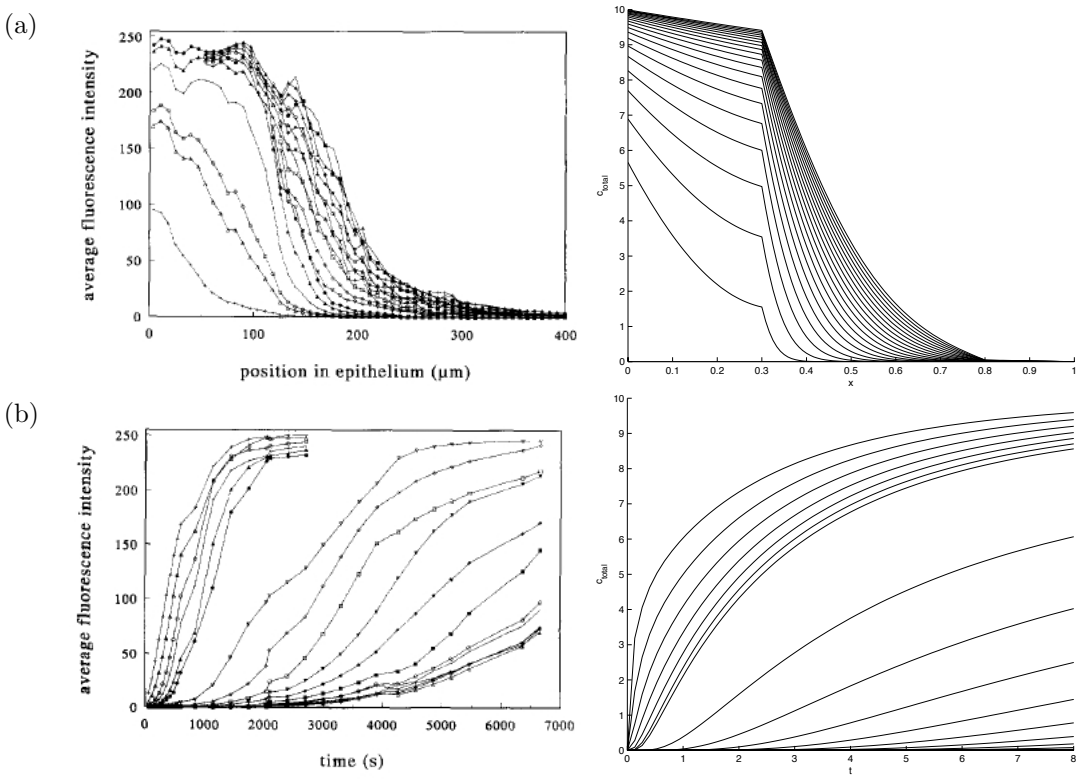

Figure 4: Comparison of simulated results (right) with data (left, repeated from Figure 2). (a) Shows the time evolution of the drug concentration (steps of $t = 20$ up to $t = 400$) and (b) shows the concentration evolution at equally spaced points (from $x = 0$ to $x = 1$ in steps of $x = 0.05$.)

includes a brief explanation of their interpretation), noting they are chosen so that equation (20) is satisfied.

Figure 4 shows a simulation that yields results qualitatively similar to the data profiles shown in Figure 2 (and reshown on the left-hand side of the current Figure). The simulated results as shown are fairly robust to the parameters changes, provided (20) holds. As noted above, the experimental results in Figure 2(b) show that the drug in the inner regions eventually reaches the maximal concentration which is the same as that in the tissue nearest to the drug source. The steady-state (linear) concentration profile descends sharply in the lipid layer, and only reaches levels of layer 1 in the very localised vicinity of $x = X_{12}$.

The evolution of drug efflux is shown in Figure (5)(a) and increases monotonically in time to a steady-level. The key information gleaned from such a graph is the timescale in which a steady-level is achieved, as this provides a timescale for which the drug needs to remain stable, i.e. the half-life of the drug needs to exceed this timescale in order to be effective. A theoretical estimate of the transit time of the drug can be estimated on the basis that the time it takes for a substance to diffuse a distance X in 1-dimension is about $X^2/2D$, with D being the diffusion coefficient; noting

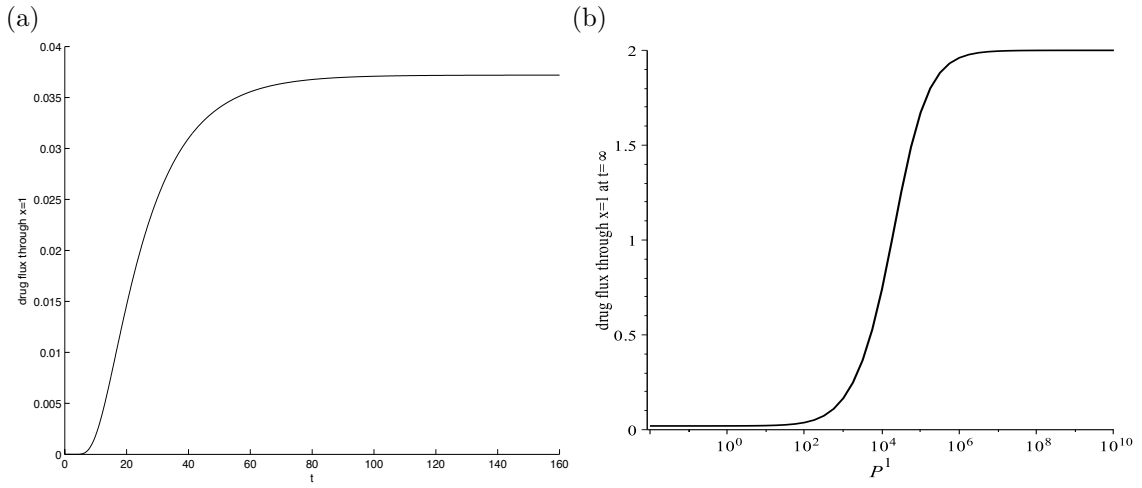

Figure 5: (a) evolution of efflux of drug ($-D_w^3\phi_w^3\partial c_w^3/\partial x|_{x=1}$) at the epithelial base and (b) the steady-state efflux as a function of P^1 (with $P^3 = P^1$ and P^2 adjusted according to (20)). Other values as listed in Table 2.

that the effective diffusion coefficient in each layer is $D_e^i = (D_W^i\mathcal{B}_W^i + D_L^iP^i\mathcal{B}_L^i)/(\phi_W^i + P^i\phi_L^i)$, the transit time T^* across the 3 layers is approximately

$$T^* = \frac{X_{12}^2(\phi_W^1 + P^1\phi_L^1)}{2(D_W^1\mathcal{B}_W^1 + D_L^1P^1\mathcal{B}_L^1)} + \frac{(X_{23} - X_{12})^2(\phi_W^2 + P^2\phi_L^2)}{2(D_W^2\mathcal{B}_W^2 + D_L^2P^2\mathcal{B}_L^2)} + \frac{(1 - X_{23})^2(\phi_W^3 + P^3\phi_L^3)}{2(D_W^3\mathcal{B}_W^3 + D_L^3P^3\mathcal{B}_L^3)}. \quad (21)$$

Using the values in Table 2 gives $T^* \approx 65.4$, which is a reasonable estimate of when the steady-state drug efflux is approximately reached. Note that no degradation is assumed in this simulation, and this will have significant impact on the results for drugs with half-lives smaller than T^*.

Figure (5)(b) shows the effect of the partition coefficient on the drug efflux through $x = 1$. This profile was generated using the steady-state solutions of equation (17). As discussed during the study group week, various experiments typically suggest a unimodal profile of drug flux against partition coefficient; the existing model as it stands cannot predict such a profile. The model correctly predicts the increase in flux as lipophilicity increases, but does not predict the descent of the profile at very high lipophilic levels. We note at extremely high lipophilicity ($P^1, P^2, P^3 \to \infty$), and with $\mathcal{B}_L^i = \phi_L^i$ and $\mathcal{B}_W^i = \phi_W^i$, the predicted transit timescale will be

$$T^* \sim \frac{X_{12}^2}{2D_L^1} + \frac{(X_{23} - X_{12})^2}{2D_L^2} + \frac{(1 - X_{23})^2}{2D_L^3},$$

so a very small D_L^i will yield a very large T^*, hence the experimental observation may simply be a case of not running the experiment for long enough.

As noted earlier, given the nature of partitioning, it seems rather extraordinary that the experimental results shown in Figure 2 indicates a monotonic profile. Figure 6 shows a simulation in which the partition coefficient in the lipid layer has been trebled, with all other parameters the same as those used in Figure 4. The lipid layer lies between 0.3 and 0.8 and in Figure 6(a) the

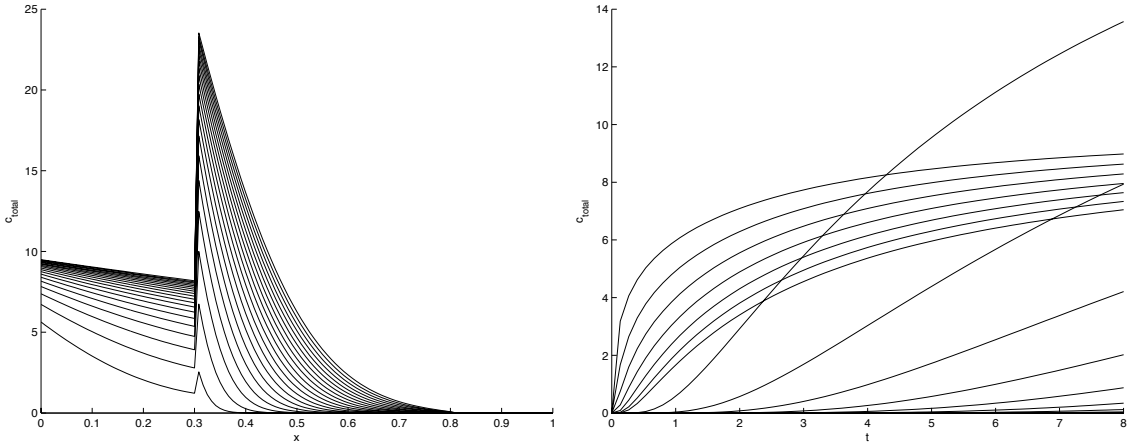

Figure 6: Repeat of simulation shown in Figure 5, except the value of P^2 has been trebled (i.e. $P^2 = 3117/49$).

expected elevation in drug concentration from $x = X_{12} = 0.3$ is observed. The profiles of the drug concentration evolution at specific points in the epithelium (Figure 6(b)) is somewhat different to the profile indicated in the data. In this simulation the lipid layer is able to harbour more of the drug than outside, hence the curves corresponding to this layer overshoot those corresponding to layer 1.

5 Conclusion and future work

The oral mucosa provides an alternative to the commonly used methods of drug delivery (this includes injections). Drug delivery via the oral mucosa has a number of advantages including the following:

- Oral cavity is well hydrated making it accessible for self administration and aids the solubility of the drug.
- Useful for chronic diseases where frequent and emergency drug administration is required (e.g. in diabetic patients or patients with heart conditions).
- Drug delivery to the bloodstream (for a quicker response).
- Harsh environment of the GI tract and first pass metabolism in the liver that prevent oral drug delivery is avoided.

Although the oral mucosa provides an ideal alternative to the current methods of drug delivery the permeability barrier plays a crucial role in its limitations.The aim of the workshop was to determine the characteristics of a drug which affected the transmucosal delivery. As the diffusion of a drug is the result of a complex combination of factors it was decided that the workshop would focus solely on lipophilicity as it is one of the most important properties. The workshop highlighted

the importance of considering the movement of a drug throughout the different portions of the epithelium to understand and predict diffusion across the mucosa. The model was able to predict behaviour seen in the experimental data reported in Hoogstraate et al (1996) as presented in Figure 4. Although there is a unmet need for further experimentation, in particular to demonstrate whether the monotonic profile of the data is a result of peculiar properties of the drug and skin used in the experiment or is in fact a seemingly universal result. In the later case, then there will be a need of a rethink of the assumptions of the current model presented here. From a modelling perspective future developments could include the following:

- Consider other relevant experimental data for comparative purposes.
- Compare the effect of drug delivery via the paracellular (around the cell) and transcellular (through the cell) routes.
- Investigate drug being internalised by cells during delivery through the oral mucosa.

Experimentally most studies looked only at the total diffusion of a substance across the whole epithelium. However, information on the flux across each layer is crucial in order to determine the contribution of each layer in the permeability barrier. Unfortunately this is challenging to measure experimentally. Future experimental investigation into the distribution of a variety of compounds through the oral mucosa over time will be useful to validate the current model and determine if varying lipophilicity alters the spatial distribution.

Acknowledgements

The authors would like to thank Dr Helen Colley, Dr Craig Murdoch and Professor Martin Thornhill from School of Clinical Dentistry at University of Sheffield for their input into developing the problem.

References

[1] Wikipedia. First pass effect. 2012. Available from http://en.wikipedia.org/wiki/First_pass_effect

[2] Hearnden, V., et al., New developments and opportunities in oral mucosal drug delivery for local and systemic disease. Adv Drug Deliv Rev, 2012. 64(1): p. 16-28.

[3] Anissimov, Y.G., et al., Mathematical and pharmacokinetic modelling of epidermal and dermal transport processes. Advanced Drug Delivery Reviews, 2012(0).

[4] Hoogstraate, A.J., et al., Diffusion rates and transport pathways of Florescien Isothiocynate (FITC)-labelled model compounds through buccal epithelium. Pharmaceutical Research, 1994. 11(1): p. 83-89.

[5] Hoogstraate, A.J., et al., A novel in-situ model for continuous observation of transient drug concentration gradients across the buccal epithelium at the microscopical level. Journal of Controlled Release, 1996. 39: p. 71-78.

[6] Galey, W.R., H.K. Lonsdale, and S. Nacht, The in vitro permeability of skin and buccal mucosa to selected drugs and tritiated water. J Invest Dermatol, 1976. 67(6): p. 713-7.

[7] Squier, C.A. and B.K. Hall, The Permeability of Skin and Oral Mucosa to Water and Horseradish Peroxidase as Related to the Thickness of the Permeability Barrier. J Investig Dermatol, 1985. 84(3): p. 176-179.

[8] Squier, C.A., et al., Oral Mucosal Permeability and Stability of Transforming Growth Factor Beta-3 In Vitro. Pharmaceutical Research, 1999. 16(10): p. 1557-1563.

[9] van Eyk, A.D. and P. van der Bijl, Comparative permeability of various chemical markers through human vaginal and buccal mucosa as well as porcine buccal and mouth floor mucosa. Arch Oral Biol, 2004. 49(5): p. 387-92.

[10] Hearnden V, Sankar V, Hull K, Juras DV, Greenberg M, Kerr AR, et al. (2012). New developments and opportunities in oral mucosal drug delivery for local and systemic disease. Adv Drug Deliv Rev 64(1):16-28.

[11] UKMi. New Drugs online. 2012. Available from http://www.ukmi.nhs.uk/applications/ndo/record_view_open.asp?newDrugID=3119

[12] McNeil Healthcare UK. 2012. Available from http://www.nicorette.co.uk/products/quick-mist

[13] Richardson G., Denuault G. & Please C.P., "Multiscale modelling and analysis of lithium-ion battery charge and discharge". *J. Eng. Math.* **72**, 4172 (2012).

[14] Maria Bruna, "Excluded-volume Effects in Stochastic Models of Diffusion". *D.Phil. Thesis*, University of Oxford (2012).

A Non-equilibrium boundary layer in the mixed region

The assumption (7) of equilibrium in the partition between the water and lipid phases in the mixed layer states that $c_L P^{-1/2} = c_w P^{1/2}$. This assumption cannot hold hold near the boundary with the lipid layer, as it is incompatible with the boundary conditions (5) and (6) imposed there.

The assumption arose because $T\gamma^2 b_{et} \gg 1$ meant that there was nothing with which to balance the partitioning terms $\pm\gamma^2 b_{et}(c_L P^{-1/2} - c_w P1/2)$ in (2) and (3) over the length and time scales of interest. However, since the boundary conditions force a different behaviour, we expect a boundary layer to form, in which the shorter length scale promotes the spatial derivatives in the diffusion terms in (2) and (3), allowing them to become large enough to balance the partitioning terms.

A.1 Boundary-layer equations

We estimate the length scale ℓ of the boundary layer by balancing the diffusion and partitioning terms in the mixed layer equations (2) and (3). It is not clear *a priori* exactly how the two diffusivities should be averaged. But it turns out that the correct length scale to chose is given by

$$\ell = \frac{1}{\gamma\sqrt{b_{et}}}\left(\frac{P^{-1/2}}{D_L\mathcal{B}_L} + \frac{P^{1/2}}{D_W\mathcal{B}_W}\right)^{-1/2} . \tag{22}$$

We then define a new dimensionless boundary-layer coordinate

$$\xi = \frac{\pm(x \mp d)}{\ell} , \tag{23}$$

where the choice of sign distinguishes between the two different mixed layers. We also write $c_L(x) = \hat{c}_L(\xi)$ an $c_W(x) = \hat{c}_W(\xi)$ in the boundary layer, to distinguish those variables from their counterparts in the bulk of the layer.

Since $4d^2\gamma^2 b_{et}/D_F \gg 1$, equations (2) and (3) reduce to

$$\left(\frac{P^{-1/2}}{D_L\mathcal{B}_L} + \frac{P^{1/2}}{D_W\mathcal{B}_W}\right) D_L\mathcal{B}_L \frac{\partial^2\hat{c}_L}{\partial\xi^2} - \left(\hat{c}_L P^{-1/2} - \hat{c}_W P^{1/2}\right) = 0 , \tag{24}$$

$$\left(\frac{P^{-1/2}}{D_L\mathcal{B}_L} + \frac{P^{1/2}}{D_W\mathcal{B}_W}\right) D_W\mathcal{B}_W \frac{\partial^2\hat{c}_W}{\partial\xi^2} - \left(\hat{c}_L P^{-1/2} - \hat{c}_W P^{1/2}\right) = 0 , \tag{25}$$

in the boundary layer, subject to the boundary conditions

$$\hat{c}_L = c_F(\pm d) , \quad D_L\mathcal{B}_L \frac{\partial\hat{c}_L}{\partial\xi} = \pm\ell D_F c_F'(\pm d) , \quad \frac{\partial\hat{c}_W}{\partial\xi} = 0 \qquad \text{at} \qquad \xi = 0 ; \tag{26}$$

$$\left(\hat{c}_L P^{-1/2} - \hat{c}_W P^{1/2}\right) \to 0 \quad \text{and}$$

$$\phi_L\hat{c}_L + \phi_W\hat{c}_W \sim c(\pm d) + \pm\ell c'(\pm d)\,\xi \qquad \text{as} \qquad \xi \to \infty . \tag{27}$$

Equations (26) arise from the matching conditions between the mixed and lipid layers. Equations (27) arise from needing to match the concentrations in the boundary layer with the concentrations in the bulk of the mixed layer. (We need to ensure equilibrium between the phases, and that we match the mean concentration $c = \phi_L c_L + \phi_W c_W$.)

A.2 General Solution

Summing equations (24) and (25) we obtain

$$\frac{\partial^2}{\partial \xi^2}\left(D_L \mathcal{B}_L \hat{c}_L + D_W \mathcal{B}_W \hat{c}_W\right) = 0\,, \tag{28}$$

which represents conservation of flux through the layer. The general solution is

$$D_L \mathcal{B}_L \hat{c}_L + D_W \mathcal{B}_W \hat{c}_W = A + B\xi\,. \tag{29}$$

Multiplying (24) and (25) by $P^{-1/2}$ and $P^{1/2}$ respectively, and then taking the difference, we obtain

$$\frac{\partial^2}{\partial \xi^2}\left(\hat{c}_L P^{-1/2} - \hat{c}_W P^{1/2}\right) - \left(\hat{c}_L P^{-1/2} - \hat{c}_W P^{1/2}\right) = 0 \tag{30}$$

which governs the deviation from equilibrium between the water and lipid components. The general solution is

$$\hat{c}_L P^{-1/2} - \hat{c}_W P^{1/2} = Re^{\xi} + Se^{-\xi} \tag{31}$$

We can use the two general solutions (29) and (31) to obtain expressions for $\hat{c}_L$ and$\hat{c}_W$ in the boundary layer:

$$\hat{c}_L = \frac{P(A + B\xi) + P^{1/2} D_W \mathcal{B}_W (Re^{\xi} + Se^{-\xi})}{P D_W \mathcal{B}_W + D_L \mathcal{B}_L}\,, \tag{32}$$

$$\hat{c}_W = \frac{(A + B\xi) - P^{1/2} D_L \mathcal{B}_L (Re^{\xi} + Se^{-\xi})}{P D_W \mathcal{B}_W + D_L \mathcal{B}_L}\,, \tag{33}$$

A.3 Applying the boundary conditions

We now apply the boundary conditions (26)–(27) to determine the four unknown constants A, B, R, S. Since there are more boundary conditions than unknowns, we will expect to also obtain constraints between the quantities $c(\pm d)$, $c'(\pm d)$, $c_F(\pm d)$, and $c'_F(\pm d)$ that appear in the boundary conditions.

Applying (27a) to (31) we find that we must have $R = 0$. Applying (27b) to (32) and (33) we find we require

$$\frac{P\phi_W + \phi_L}{P D_W \mathcal{B}_W + D_L \mathcal{B}_L}(A + B\xi) \sim c(\pm d) \pm \ell c'(\pm d)\,\xi \quad \text{as} \quad \xi \to \infty \tag{34}$$

Hence

$$A = D_e\, c(\pm d)\,, \qquad B = \pm \ell D_e\, c'(\pm d)\,, \tag{35}$$

where D_e is the effective diffusivity, as defined in (9).

Applying (26c) to (33) we find

$$B + P^{1/2} D_L \mathcal{B}_L S = 0\,, \tag{36}$$

and hence

$$S = \mp \frac{\ell D_e\, c'(\pm d)}{P^{1/2} D_L \mathcal{B}_L}\,. \tag{37}$$

The four constants of integration have now all been found, so applying the remaining conditions will provide constraints on the bulk quantities. Applying (26b) and (26c) to (29) we obtain

$$B = \pm \ell D_F \, c'_F(\pm d) \, . \tag{38}$$

Comparing the two expressions for B, we must therefore have

$$D_e \, c'(\pm d) = D_F \, c'_F(\pm d) \, . \tag{39}$$

Applying (26a) to (32) we find that we must have

$$c_F(\pm d) = \frac{PA + P^{1/2} D_W \mathcal{B}_W S}{P D_W \mathcal{B}_W + D_L \mathcal{B}_L} \, , \tag{40}$$

and hence

$$c_F(\pm d) = \frac{1}{\phi_L + P^{-1} \phi_W} \left[c(\pm d) \mp \frac{\ell D_W \mathcal{B}_W}{P D_L \mathcal{B}_L} c'(\pm d) \right] \tag{41}$$

A.4 Effective conditions on the bulk solutions

The two constraints (39) and (41) provide the effective boundary conditions on the bulk solutions either side of the boundary layer. Equation (39) is used unmodified, and represents the conservation of flux into and out of the (quasi-steady) boundary layer.

For (41) we assume that

$$\frac{D_W \mathcal{B}_W \, \ell}{D_L \mathcal{B}_L \, P d} \ll 1 \, , \tag{42}$$

where d is the length scale of the bulk solution. Then we can neglect the term involving c' and the condition reduces to

$$c_F(\pm d) = \frac{c(\pm d)}{\phi_L + P^{-1} \phi_W} \, . \tag{43}$$

The assumption (42) means that the change in concentration in the lipid phase across the boundary layer is small. This is achieved by having a thin boundary layer ($\ell / L \ll 1$). Higher lipophilicities ($P \geq O(1)$) also help as then more mass is already present in the lipid layer. These effects must be enough to overcome the fact that ($D_W \gg D_L$).